of their scanning calorimetric experiments with human albumin. We express thanks to Enrico Di Cera regarding evaluation of the heat capacity under limiting ligand conditions and to Alfredo Colosimo, who provided assistance in the simulation of lysozyme denaturation.

Registry No. NAG_3, 38864-21-0; O_2, 7782-44-7; lysozyme, 9001-63-2.

REFERENCES

Ackers, G. K. (1979) *Biochemistry 18*, 3372-3380.
Ackers, G. K., Benesch, R. E., & Edalji, R. (1982) *Biochemistry 21*, 875-879.
Antonini, E., & Brunori, M. (1971) *Haemoglobin and Myoglobin in Their Reactions with Ligands*, North-Holland, Amsterdam.
Bannerjee, S. K., & Rupley, J. A. (1973) *J. Biol. Chem. 248*, 2117-2124.
Benesch, R., Benesch, R. E., & Yu, C. I. (1968) *Proc. Natl. Acad. Sci. U.S.A. 59*, 526-532.
Doyle, M. L., Di Cera, E., Robert, C. H., & Gill, S. J. (1987) *J. Mol. Biol. 196*, 927-934.
Gill, S. J., Richey, B., Bishop, G. A., & Wyman, J. (1985) *Biophys. Chem. 21*, 1-14.
Herzfeld, J., & Stanley, H. E. (1974) *J. Mol. Biol. 82*, 231-265.
Hill, T. (1986) *Cooperativity Theory in Biological Systems*, Springer-Verlag, Heidelberg.
Imai, K. (1982) *Allosteric Effects in Human Haemoglobin*, Cambridge University Press, Cambridge.
Imai, K., & Tyuma, I. (1973) *Biochim. Biophys. Acta 293*, 290-294.
Imaizumi, K., Imai, K., & Tyuma, I. (1979) *J. Biochem. (Tokyo) 86*, 1829-1840.
Imaizumi, K., Imai, K., & Tyuma, I. (1982) *J. Mol. Biol. 159*, 703-719.
Kister, J., Poyart, C., & Edelstein, S. J. (1987) *Biophys. J. 52*, 527-535.
Kister, J., Poyart, C., & Edelstein, S. J. (1988) *Biophys. J.* (Erratum) (in press).
Pace, C. N., & McGrath, T. (1980) *J. Biol. Chem. 255*, 3862-3865.
Privalov, P. L., & Khechinashvili, N. N. (1974) *J. Mol. Biol. 86*, 665-685.
Robert, C. H., Fall, L., & Gill, S. J. (1988) *Biochemistry* (following paper in this issue).
Schellman, J. A. (1975) *Biopolymers 14*, 999-1018.
Shrake, A., & Ross, P. (1987) *Abstracts of the Calorimetry Conference*, University of Colorado, Boulder, CO.
Szabo, A., & Karplus, M. (1976) *Biochemistry 15*, 2869-2877.
Velicelebi, G., & Sturtevant, J. M. (1979) *Biochemistry 18*, 1180-1186.
Wyman, J. (1964) *Adv. Protein Chem. 19*, 223-286.
Wyman, J. (1965) *J. Mol. Biol. 11*, 631-644.
Wyman, J. (1967) *J. Am. Chem. Soc. 89*, 2202-2218.
Wyman, J. (1984) *Q. Rev. Biophys. 17*, 453-488.
Wyman, J., & Gill, S. J. (1975) *Proc. Natl. Acad. Sci. U.S.A. 77*, 5239-5242.

Linkage of Organic Phosphates to Oxygen Binding in Human Hemoglobin at High Concentrations†

Charles H. Robert,‡ Lana Fall, and Stanley J. Gill*
Department of Chemistry and Biochemistry, University of Colorado, Boulder, Colorado 80309-0215
Received January 8, 1988; Revised Manuscript Received March 30, 1988

ABSTRACT: We have performed high-precision oxygen binding studies on human hemoglobin tetramers in the presence of a series of limited, subsaturating amounts of the effector compounds 2,3-diphosphoglycerate (DPG) and inositol hexaphosphate (IHP). The use of thin-layer optical methods enabled the use of high hemoglobin concentrations, preventing complications arising from the dissociation of the tetramer into dimers. Model-independent, simultaneous analysis of all data for each effector demonstrated that the intrinsic oxygen binding characteristics of the molecule are in agreement with those determined in earlier high-precision studies [e.g., Gill, S. J., Di Cera, E., Doyle, M. L., Bishop, G. A., & Robert, C. H. (1987) *Biochemistry 26*, 3995-4002] and that the affinity of the tetramer for the tightly binding effector IHP changes most markedly between the second and fourth oxygen binding steps, perhaps indicating a large conformational change. The data were then analyzed by using the truncated allosteric model [Di Cera, E., Robert, C. H., & Gill, S. J. (1987) *Biochemistry 26*, 4003-4008], which is based on the hypothesis that a quaternary conformational change occurs in the hemoglobin tetramer before the third and fourth oxygen molecules bind.

Organic phosphates are well-known regulators of the oxygen binding affinity of human hemoglobin. Of the physiological effectors, 2,3-diphosphoglycerate (DPG) is of primary importance (Benesch et al., 1968, 1971), while of the non-endogenous compounds, inositol hexaphosphate (IHP) has proven valuable because of its strong linkage. These compounds bind with a stoichiometry of one molecule per hemoglobin tetramer (Benesch et al., 1968, 1971; Janig et al., 1971; Edalji et al., 1976) and are thought to bind at the same site. It is likely that the mechanisms of their linkage to oxygen binding are similar as well. Their study can be seen to be especially germane when one considers that the ligand binding site, situated between the β-chain termini of the $\alpha_2\beta_2$ tetramer (Arnone, 1972; Arnone & Perutz, 1974; Perella et al., 1975;

† This work was supported by National Institutes of Health Grant HL 22325.
* To whom correspondence should be addressed.
‡ This work was performed in partial fulfillment of requirements for the Ph.D. degree in Chemistry and Biochemistry at the University of Colorado, Boulder, CO.

0006-2960/88/0427-6835$01.50/0

Gupta et al., 1979), occupies a nearly central position among the four oxygen binding sites; thus, changes in the tightness of the binding of organic phosphate in the intermediate stages of oxygen binding will reflect the tetramer's cooperative changes, presumably at both the quaternary and the tertiary level. The precise study of such simple linkage systems is the logical extension of studies of oxygen binding alone, enabling additional insights to be gained into the allosteric mechanisms of cooperativity.

Determination of the relative binding constants for DPG and IHP to hemoglobin in intermediate oxygenation states has been attempted from whole-curve analyses (Tyuma et al., 1973), but those studies were carried out under conditions where the concentration of the second ligand was in large excess over that of the hemoglobin molecule and thus by necessity only low hemoglobin concentrations could be employed, causing some problems with overall consistency, as pointed out by Szabo and Karplus (1976). Subsequent studies at higher concentration (Imaizumi et al., 1979) provided intermediate values for DPG binding alone. Nevertheless, high hemoglobin concentrations provide two benefits: The first is achieving conditions where tetramer dissociation effects are negligible (Ackers et al., 1975; Johnson & Ackers, 1977), thus enabling simplification of the data analysis; the second is the attainment of near physiological conditions, where organic phosphates may not be present in saturating amounts.

Subsaturating organic phosphate conditions are known to produce striking effects in the oxygen binding curve, which can become biphasic (Benesch et al., 1968). The increased structure of the curves increases the potential for resolution of the binding constants for hemoglobin in the intermediate oxygenated states. The situation has been explored in part by Ackers, who formulated the dependence of the median oxygen pressure of binding curves on the total amount of organic phosphate present (Ackers, 1979). Imai and Tyuma (1973) showed, through simulation, the effects of near equimolar concentrations of the organic phosphate on the oxygen binding curve. Attempts at full analysis of the oxygen binding reactions of hemoglobin in the presence of limited total amounts of organic phosphates have been made, first by Herzfeld and Stanley (1974) and recently by Kister et al. (1987a,b). However, in those studies low hemoglobin concentrations were used and there was no model-independent analysis of the binding data, which would have enabled comparison to earlier studies.

In this paper we report high-precision oxygen binding data obtained with a thin-layer apparatus (Dolman & Gill, 1979; Gill et al., 1987) at high, nearly physiological concentrations of hemoglobin for a wide range of Hb/organic phosphate molar ratios. The accompanying paper (Robert et al., 1988) treats the general problem of the influence of a second ligand present in limited quantity on the binding curve of the primary ligand; here we apply the formulation to single-site binding of the second ligand, the case for DPG or IHP. The data presented are analyzed in a simultaneous fitting procedure enabling extraction of the oxygen and phosphate binding constants. We conduct the analysis first in the context of the model-independent Adair formulation and then in the context of a simple modification (Di Cera et al., 1987) of the familiar Monod, Wyman, and Changeux (MWC) model (1965) that has found success in uniting diverse aspects of the existing structural results and high-precision functional data for human hemoglobin (Di Cera et al., 1987; Doyle et al., 1987a,b). The present study was designed to avoid pitfalls encountered in previous work, the most recent being that of Kister et al. (1987a,b): (1) Our binding measurements involved the evaluation of, essentially, the derivative of the binding curve at a series of equilibrium points. The derivative procedure provides advantages by simplification of the fitting problem (Sturgill & Biltonen, 1978) and by elimination of the classical problem of evaluation of asymptotical limits of the binding curve. (2) Model-independent analysis was performed in order to compare derived parameters to those obtained in other studies present in the literature. (3) High concentrations of hemoglobin, nearing physiological conditions, were employed to avoid the complicating effect of the dimer–tetramer equilibrium encountered with low concentration studies (Ackers et al., 1975), which may actually be increased in the presence of DPG (Benesch et al., 1986).

Materials and Methods

Solutions. All hemoglobin samples used in this study were given to our laboratory by Dr. Bo Hedlund (University of Minnesota) after preparation by the method of Williams and Tsay (1973) with phosphates stripped on a DEAE-25 ion-exchange column. The purified hemoglobin (16 mM heme), obtained in distilled, deionized water, was frozen in drops in liquid nitrogen and stored in sealed vials in liquid nitrogen until use.

Hemoglobin stock solutions were prepared from thawed drops by dilution with an equal volume of twofold concentrated HEPES buffer, salt, and enzymatic reducing system (Hayashi et al., 1973). IHP and DPG stock solutions were prepared in buffer from fresh material (Sigma Chemical Co.; sodium salts) by using the hydrated weights for concentration determination. We used HCl to adjust the pH of IHP or DPG stock solutions (20 mM) to that of the Hb solution, monitoring the volume of HCl added in order to be sure of the total 0.1 M Cl^- in final solutions. pH's of final sample solutions were checked and where necessary small adjustments made using the small-volume pH titrator developed by Spokane et al. (1980).

The final sample solutions were made by combining the Hb stock solution (2 mM tetramer) with dilutions of the IHP or DPG stock solutions such that equal volumes produced the desired final concentrations of both Hb and IHP or DPG. Final conditions for all experiments were 1 mM Hb tetramer, 0.1 M HEPES buffer solution, and 0.1 M total Cl^-. The reducing system limited metHb (oxidized Hb) concentrations to levels less than 3% in all runs tested as determined by the ratio of absorbances at 577 and 500 nm (Kilmartin et al., 1978). The met ratio test was not applied to runs conducted in the presence of IHP due to the effect of this compound on the optical spectra of hemoglobin; in any event, these runs required less time under oxidizing conditions (25 °C) than any others.

Oxygen Binding Curves. We used the Gill thin-layer optical cell (Dolman & Gill, 1978) for oxygen binding measurements. With this method a thin layer of the sample is sandwiched between the glass window and a gas-permeable membrane (General Electric Spectra-pore MEM-13) in contact with a gas reservoir, which itself is optionally connected to the bore volume of a stainless steel stopcock. Sample layer thickness in most experiments was 0.005 cm (0.002 in.). A thermostat-controlled water bath maintained cell temperature at 25.0 ± 0.02 °C. In these experiments the cell is initially flushed and equilibrated with starting gas (here pure oxygen). The starting gas is then diluted by turning the stopcock—thus connecting the stopcock bore, which has been flushed with pure nitrogen. Typically, the absorbance (577 nm in these experiments) is monitored on a strip chart of a Cary 219 spec-

trophotometer throughout to verify equilibration. The dilutions are repeated in a stepwise fashion to traverse the binding curve. The absorption differences, corrected as needed for any slight drift, make up the experimental measurements. Total pressure at all times is atmospheric (in Boulder, ~630 Torr).

Oxygen pressures in the thin-layer cell are determined by the dilution equation for the device:

$$p_i = p_0 D^i \tag{1}$$

where p_i is the oxygen pressure at step i, p_0 is the starting oxygen pressure, determined barometrically, and D is the dilution factor (typically ~0.698 with an error of 0.0003 in a run). The factor D depends on the precise geometry of the cell and bore; we determine it for each run by nonlinear least-squares fitting of eq 1 to stepwise readings from an oxygen electrode (Yellow Springs Instruments, Yellow Springs, OH) residing in the stopcock assembly.

Data Analysis. One fits the sequential changes in the absorbance, ΔA, of the sample layer with

$$\Delta A(x_i,y_i) = [\theta(x_i,y_i) - \theta(x_{i-1},y_{i-1})]\cdot\Delta A_{\text{total}} \tag{2}$$

where ΔA_{total} is the hypothetical absorbance change for complete saturation of the unsaturated macromolecule (thus, a fitting parameter) and θ is the ligand saturation of the macromolecule at primary ligand X (oxygen) activity x and second ligand Y (IHP or DPG) activity y. The activity of X is measured in units of the partial pressure of the gaseous oxygen. The fractional saturation is the average saturation divided by the number of sites, so

$$\theta = \frac{\bar{X}}{4} = \tfrac{1}{4}\left[\frac{\partial \ln P(x,y)}{\partial \ln x}\right]_y \tag{3}$$

where P is the binding polynomial (Wyman, 1948)—the binding partition function—as discussed in the preceding paper and given in the next section for the present application. The activity of the second ligand (y) at a given x activity is given by solution of general eq 8 in the preceding paper (Robert et al., 1988), which reduces to a quadratic in y for the one-to-one stoichiometry of Y binding in the present case, eq 10 of that paper.

In addition to the total optical density change, the various binding constants for oxygen and the organic phosphates constitute the fitting parameters. An overall 1% correction, linear with the extent of oxygenation, was applied in the fitting function to take into account the spectral change resulting from the binding of IHP (Adams & Schuster, 1974; Imai, 1978). The effect of the correction for data obtained with DPG was small enough to be neglected. Parameters were determined from the data by nonlinear least-squares fitting of eq 3 using the Gauss–Newton method as modified by Marquardt (1963) and others (Magar, 1972). F tests were used for determination of 1 SD (67%) confidence intervals on critical parameters. All analyses were performed with Hewlett-Packard 9816 or 310 computers.

Graphic representation of the finite differences function in eq 2 was obtained through expression at any step i of the previous ligand activity, x_{i-1}, in terms of the dilution factor D ($x_{i-1} = x_i/D$). The entire curve was thus repesented as a smooth function of a single variable. The finite difference approximation of the derivative of θ with respect to the logarithm of the x activity is best placed at the midpoint of the logarithmic step in x activity; $\log \xi_i = 0.5(\log x_i + \log x_{i-1})$; or $\xi = x/\sqrt{D}$, the corresponding midpoint activity.

Application of the Adair Approach and the Modified MWC Model. Since the binding partition function P is the sum of species in the system at equilibrium, it follows that writing it

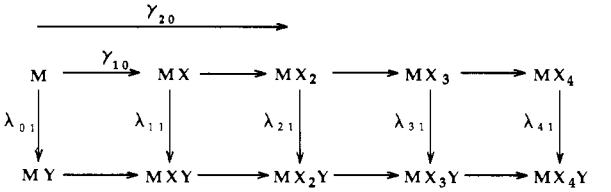

FIGURE 1: Array of stoichiometric (Adair) species for hemoglobin binding of oxygen (X) and organic phosphate (Y = DPG or IHP).

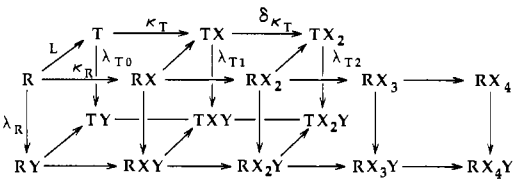

FIGURE 2: Array of species for the truncated MWC model (Di Cera et al., 1987) in which the β chains are blocked with respect to oxygen in the T (deoxy) form of the hemoglobin molecule.

incorporates the particular thermodynamic model for the binding process. Although, strictly, the Adair scheme (Adair, 1925) is a "model", its tenets, simply the tetrameric nature of the molecule with respect to oxygen binding sites and the one-to-one stoichiometry of IHP or DPG binding, are so well established that we call it here the model-independent scheme. [Such would not be the case at lower concentrations, where the dimer–tetramer equilibrium would have to be considered; see, for example, Ackers et al. (1975).] We also examine the data in the context of the model presented in Di Cera et al. (1987a), which draws together oxygen binding data and structural data for human hemoglobin.

Adair Scheme. The macromolecular species considered in the Adair approach appear in Figure 1. As is evident, only the stoichiometric species are considered. Y indicates effector molecules; X indicates oxygen. The binding polynomial is the sum of the equilibrium concentrations of these species (relative to the unligated species), which we write in terms of the mass laws governing the overall oxygen binding reactions M + iX $\rightarrow$ MX$_i$ with equilibrium constant γ_{i0} and the phosphate binding constants λ_{i1} for the reactions MX$_i$ + Y $\rightleftharpoons$ MX$_i$Y. As was done in the preceding paper, the X binding subpolynomials are written $P_0(x)$ and $P_1(x)$, the first summing over oxygen binding of the Y free species and the second summing over the oxygen binding of the Y ligated species. Thus, the binding polynomial can be written

$$P = P_0(x) + yP_1(x) \tag{4}$$

where

Adair scheme

$$P_0(x) = 1 + \gamma_{10}x + \gamma_{20}x^2 + \gamma_{30}x^3 + \gamma_{40}x^4 \tag{5}$$

and

$$P_1(x) = \lambda_{01} + \lambda_{11}\gamma_{10}x + \lambda_{21}\gamma_{20}x^2 + \lambda_{31}\gamma_{30}x^3 + \lambda_{41}\gamma_{40}x^4 \tag{6}$$

for the oxygen binding properties of the molecule without and with effector bound, respectively. The desired equation for $\theta_{\text{Adair}}(x,y)$ is obtained by operating on P as shown by eq 3. As stated above, the free activity y of the effector is found by solution of eq 10 in the preceding paper.

Application of the Truncated Allosteric Model. Figure 2 shows the species hypothesized in the modification of the MWC model proposed by Di Cera et al. (1987a). The key element of this model is the truncation of the oxygen binding stoichiometry in the "T" or deoxy state: The β chains are considered to be blocked in solution by Val-E11 so that binding

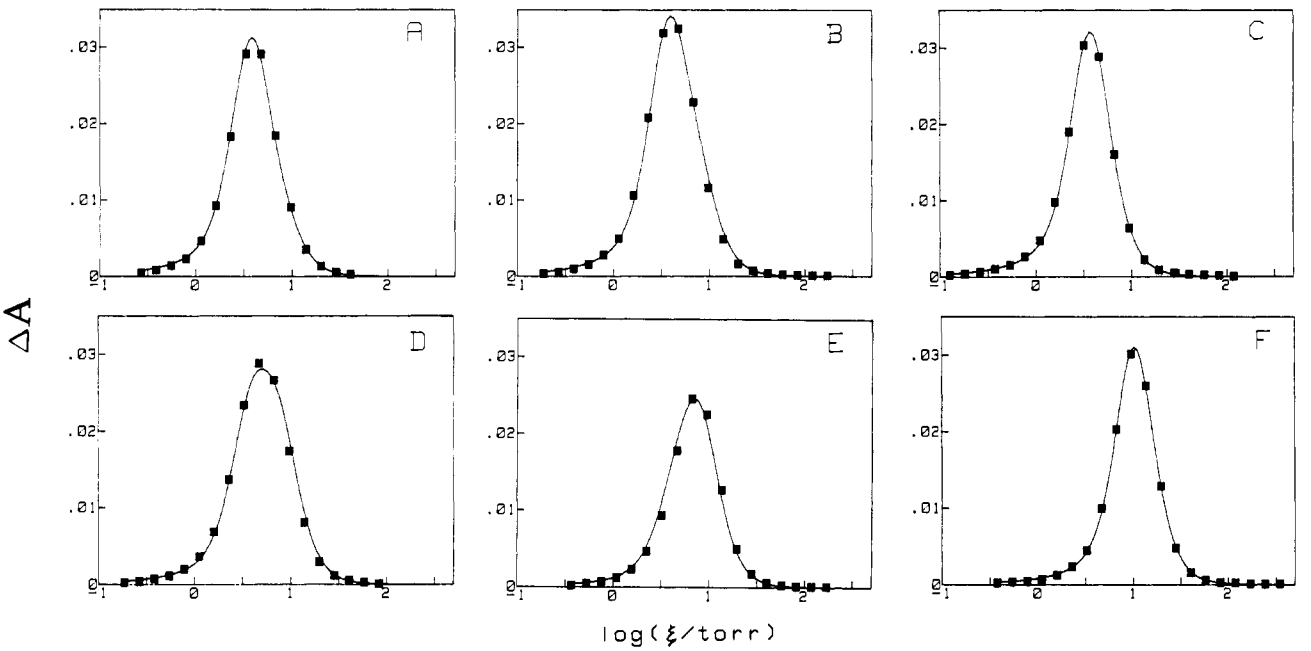

FIGURE 3: Binding capacity data obtained with the effector DPG. Hb tetramer concentration 0.001 M, 0.1 M HEPES, pH 7.47, 25 °C, and 0.1 M total chloride; DPG concentrations for panels A–F are 0, 0.0001, 0.0002, 0.0005, 0.001, and 0.010 M, respectively.

occurs to only the two α chains in the T state. Incorporated into Figure 2 are the effector-bound species, together with the definitions of the effector binding constants. It can be seen that the "R" or high-affinity state of the macromolecule in this model shows only one affinity for the second ligand; that is, the effector ligand is not linked to oxygen binding in the R state. Such an approximation, shown appropriate in fitting the data, may reflect the low population of the R0, R1, R2, and R3 oxygenated forms of the molecule and their relative inconsequence to the effect of IHP or DPG binding. In the T state the effector is linked to oxygen binding, as can be seen from the three distinct Y binding constants hypothesized for this form.

The binding polynomial for the model system is most easily written in a fashion similar to that of the Adair case: P is assembled as in eq 4 where here the binding subpolynomials can be written

truncated allosteric model

$$P_0(x) = (1 + \kappa_R x)^4 + L(1 + 2\kappa_T x + \delta\kappa_T^2 x^2) \quad (7)$$

and

$$P_1(x) = \lambda_R(1 + \kappa_R x)^4 + L(\lambda_{T0} + 2\lambda_{T1}\kappa_T x + \delta\lambda_{T2}\kappa_T^2 x^2) \quad (8)$$

which again represent the oxygen binding of the macromolecule without and with effector bound, and the equilibrium constants are defined by Figure 2. The binding constant for oxygen in the T state (κ_T) is that of the α chains. It will be noticed that the model includes a "nested" cooperative interaction (Robert et al., 1987) between the α chains in the T state, which is particularly significant ($\delta \gg 1$) in the case of carbon monoxide binding (Di Cera et al., 1987). Again, we use eq 3 to obtain $\theta(x,y)$ for this model. The free effector concentration (y) is again obtained by eq 10 in the preceding paper. The number of binding constants (thus, fitting parameters) can be seen to be one less than in the general Adair case; the model therefore simplifies the phenomenological approach.

RESULTS

We conducted binding curves for a range of organic phosphate concentrations, 0, 0.1, 0.2, 0.5, 1.0, and 10 mM, for both DPG and IHP, with a fixed hemoglobin concentration (1 mM tetramer) throughout, in 0.1 M HEPES buffer and 0.1 M total chloride, pH 7.47. HEPES buffer was chosen for the similarity of its pK_a to the experimental pH we desired; maximum buffering power is particularly important with high hemoglobin concentrations. The binding data, taken as changes in absorbance resulting from a given deoxygenation step, are presented in Figures 3 and 4 together with a smooth presentation of the finite-difference fitting function, eq 2. This function is to first order the first derivative of the binding curve and thus is an approximate measure of the "binding capacity" of the macromolecule (Di Cera et al., 1988). The behavior of the oxygen binding curves under limited concentrations of the tight binding effector IHP is striking (Figure 4). This characteristic is less evident in the case of the weaker binding compound DPG (Figure 3), although under conditions in which the hemoglobin molecule is stripped of chloride, the binding of DPG is apparently tight enough to result in biphasic curves (Imai & Tyuma, 1973).

Table I summarizes the binding parameters determined by simultaneous fitting of each series of experiments (DPG or IHP) with the Adair scheme. At the top we show the oxygen binding constants obtained from the simultaneous fitting as well as those obtained from individual fits of the blank runs (no effector present). It may be noted that the asymmetrical error ranges assigned to parameters in this table are the true confidence limits corresponding to ~1 SD as determined by application of the F test to the data fits obtained for a series of values of each parameter around the least-squares minimum, a more accurate determination than the commonly used linear approximation as pointed out by Magar (1972) and by Johnson (1981). The values obtained from the individual fits of the blank runs are not significantly different from each other or from those values determined by fitting all data simultaneously for a given compound. The simultaneous fitting of a number of data sets taken under a variety of conditions places a high demand on the consistency among all data sets. As can be seen by the results of this fit (Figures 3 and 4), the data are remarkably self-consistent. The standard errors of a point for the data fitting, expressed in absorbance units, are given in the bottom row of the table. These errors are consistent with

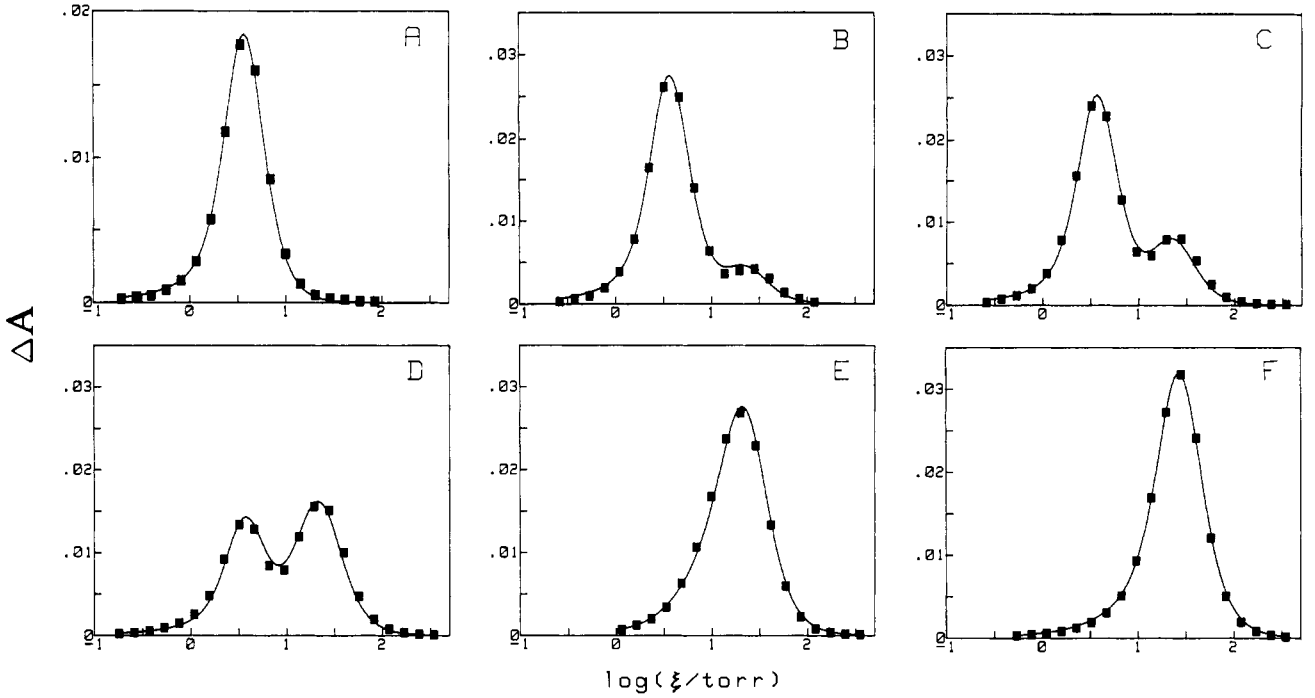

FIGURE 4: Binding capacity data obtained with the effector IHP. Experimental conditions are as in the legend of Figure 3. IHP concentrations for panels A–F are 0, 0.000 13, 0.000 24, 0.000 55, 0.001 05, and 0.0105 M, respectively.

Table I: Results of Phenomenological (Adair) Analysis

	blanks		DPG[a]	IHP[a]
γ_{10} (Torr^{-1})	0.18 (0.13, 0.25)[b]	0.144 (0.12, 0.19)	0.184 (0.11, 0.31)	0.190 (0.11, 0.29)
γ_{20} (Torr^{-2})	0.016 (0.011, 0.020)	0.016 (0.006, 0.019)	0.013 (0.0031, 0.017)	0.011 (0.001, 0.019)
γ_{30} (Torr^{-3})	0[c] (0, 0.003)	0[c] (0, 0.002)	0[c] (0, 0.002)	0[c] (0, 0.003)
γ_{40} (Torr^{-4})	0.00221 (0.0019, 0.0027)	0.00193 (0.0018, 0.0021)	0.00216 (0.0017, 0.0029)	0.00236 (0.0019, 0.0027)
λ_{01} (M^{-1})			3.4×10^4 ($3.1, 4.8$)	4.1×10^6 ($2.7, 6.2$)
λ_{11} (M^{-1})			9×10^3 ($6, 12$) $\times 10^3$	6×10^5 ($4, 13$) $\times 10^5$
λ_{21} (M^{-1})			4×10^3 ($0, 44$) $\times 10^3$	3×10^5 ($2, 9$) $\times 10^5$
λ_{31} (M^{-1})			[d]	[d]
λ_{41} (M^{-1})			400 (280, 560)	1.6×10^3 ($1.1, 2.2$) $\times 10^3$
σ[e]	2.0×10^{-4}	9.1×10^{-5}	5.3×10^{-4}	4.8×10^{-4}

[a] Simultaneous data fits of blank run and series of runs varying total [effector]. [b] 67% confidence intervals determined by F tests. [c] Sum-of-squares error was smallest with this parameter set to zero. [d] Parameter not defined due to negligibility of γ_{30}. [e] Standard error of a point is reported in absorbance units.

the precision of the spectrophotometer and variations seen between fits of repeat runs. Plots of the residuals (fitted value − observed value) of the fits are given in Figure 5. For each effector the scatter of the data points around the fitting function shows no systematic deviation.

The equilibrium constants for the binding of the organic phosphates to the stoichiometric oxygenated species are given in the bottom of Table I. The values for DPG and IHP are seen to be quite different in overall magnitude, and the tightness of binding of IHP is what causes the extreme biphasic behavior of these curves, manifested in the derivative plots as "double hump" behavior (see Figure 4).

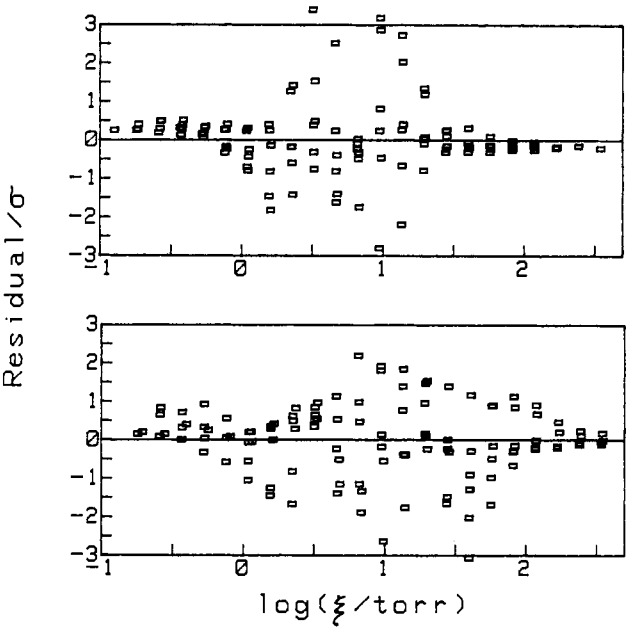

FIGURE 5: Residuals obtained in the simultaneous fitting of DPG (top panel) and IHP (bottom panel) binding capacity data, normalized to the standard error of a point for the two global fits.

Application of the truncated allosteric model (Di Cera et al., 1987a) allowed evaluation of values for the equilibrium constants describing the binding reactions that are shown schematically in Figure 2. These constants are given in Table II, where the standard errors of a point for the fits are seen to be not significantly different from those obtained by the phenomenological treatment, indicating the fitness of the model in describing the data. The fits provided by the model fitting function are not shown since they essentially overlap those of the phenomenological function shown in Figures 3 and 4.

Discussion

Analysis of Oxygen Binding Curves with Limited Total Quantities of Effector. The oxygen binding curves obtained from the derivative data shown in Figures 3 and 4 are shown

Table II: Application of Truncated Allosteric Model

	DPG[a]	IHP[a]
κ_R ($Torr^{-1}$)	20	21
	(4, *b*)	(5, *b*)
κ_T ($Torr^{-1}$)	0.10	0.10
	(0.05, 0.14)	(0.04, 0.18)
L	8×10^7	8×10^7
	(1×10^5, *b*)	(3×10^5, *b*)
δ	1.1	0.9
	(0.1, 3.5)	(0.08, 1.9)
λ_R (M^{-1})	370	1600
	(290, 550)	(1200, 2200)
λ_{T0} (M^{-1})	3.0×10^4	4.1×10^6
	$(2.4, 5.1) \times 10^4$	$(2.7, 6.1) \times 10^6$
λ_{T1} (M^{-1})	9×10^3	6.3×10^5
	$(3, 16) \times 10^3$	$(3.5, 12) \times 10^5$
λ_{T2} (M^{-1})	3.5×10^3	3.5×10^5
	$(0, 38) \times 10^3$	$(1 \times 10^5, 10^{10})$
σ[c]	5.2×10^{-4}	4.6×10^{-4}

[a] Simultaneous data fits of blank run and series of runs varying total [effector]. [b] κ_R and L are too highly correlated for accurate determination of upper confidence limits. [c] Standard error of a point is reported in absorbance units.

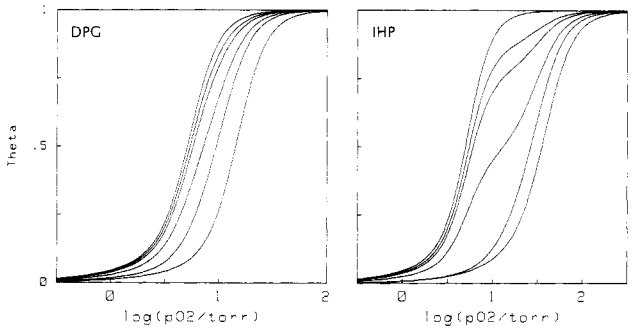

FIGURE 6: Depiction of oxygen binding curves for human hemoglobin drawn with the constants obtained from simultaneous fits of the DPG (left) and IHP (right) series of experiments shown in Figures 3 and 4.

together in Figure 6 for both DPG and IHP as the second ligand. The complex shapes of these oxygen binding curves, particularly those with IHP present, highlight the importance of complete analysis to establishing the actual behavior of macromolecules under nearly physiological conditions. The general treatment outlined in the preceding paper (Robert et al., 1988) and its successful application to the hemoglobin system here demonstrate that the complex behavior of macromolecules in equilibrium with limiting amounts of linked ligands can be taken into account in a precise way.

The binding curves shown in Figure 6 correspond to a series of parallel cuts through a thermodynamic surface of θ expressed in terms of the independent variables of the logarithm of the primary ligand X (oxygen) activity and the total concentration of Y (IHP or DPG). An example of this surface for Y = IHP is shown in the accompanying paper to illustrate the general treatment of the limited second ligand problem. The actual binding data obtained by the thin-layer equilibrium method (Dolman & Gill, 1978) correspond very closely to the derivative of the θ surface with respect to the logarithm of the oxygen activity, the "binding capacity" derivative (Di Cera et al., 1988). This derivative surface is shown in Figure 7 for the case of IHP as the second ligand. The experimental data shown in Figure 4 can be seen to correspond to vertical cuts (noted by arrows) through this surface parallel to the front axis.

The negligibility of the triply ligated species in these experiments, even to the level of precision seen in fitting an

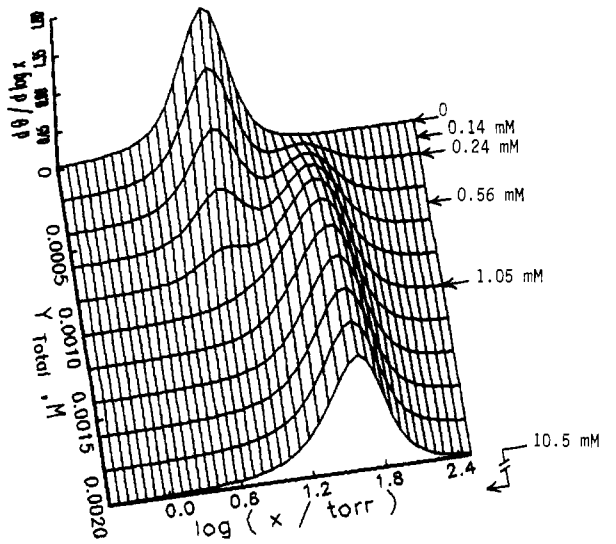

FIGURE 7: Surface depicting the derivatives of θ_{O_2} with respect to the logarithm of the oxygen activity (x), plotted as a function of log x and the total amount of effector present, in this case IHP. The corresponding θ surface for this example is shown in the preceding paper (Robert et al., 1988).

individual blank curve (0.2% of the total saturation change), is in agreement with other studies from this laboratory (Gill et al., 1987; Doyle et al., 1987; Parody-Morreale et al., 1987; Di Cera et al., 1987). In 1979, L.F., motivated by discussions with Ackers [see Ackers (1979)], conducted a series of experiments similar to those reported here using phosphate buffer (unpublished data), but the results were not fully analyzed. Analysis of those curves by the methods reported here reveals similar characteristics, notably with respect to the negligibility of the triply ligated species. The relevant aspect of the data that persists, as exemplified by the data presented in Figures 3 and 4, is the rather sudden and steep onset of absorbance changes that occur as the system is deoxygenated in a stepwise fashion. That the low triply oxygenated species would freely appear from analysis of such varied binding curves suggests an intrinsic molecular mechanism that gives rise to the strong asymmetry of the oxygen binding curve of human hemoglobin.

Table III serves to compare the effector binding constants that were determined through the methods of the present study (shown in Table I) to those existing in the literature. In the past, determinations of effector binding (see references in Table III) could be placed roughly into two classes: those determined by direct methods, such as gel filtration or pH titration, and those determined indirectly through linkage studies with oxygen binding under the assumption of fixed effector activity. Experiments of the first type have been essentially limited to measurement of either the deoxy or oxy binding constants (λ_{01} or λ_{41}). The experiments of the second type have been limited to fairly low hemoglobin concentrations in order to ensure constancy of the effector concentrations throughout the binding curve. In contrast, the method we present here and in the accompanying paper is distinctive in that it enables one to measure the equilibrium constants of the effector binding to the deoxy and oxy species as well as the intermediates under nearly physiological hemoglobin concentrations.

As seen in Table III, there is only one study (Imaizumi et al., 1979) with which one can compare our determinations of the strength of effector binding to hemoglobin in intermediate stages of oxygenation. Further, these values can be compared only for the case of DPG. They are in essential agreement within confidence intervals. Discrepancy seen between these studies probably arises from the presence in our study of

Table III: Relation to Existing Determinations[a]

λ_0	λ_1	λ_2	λ_3	λ_4	[heme]	pH	buffer	ref
				DPG				
2.5×10^4					5	7.4	Bis-Tris	*b*
1×10^5					0.3	7.3	Bis-Tris	*c*
2.4×10^4				400	2.4/16	7.2	Bis-Tris	*d*
8.2×10^4	2.0×10^3	5.6×10^3	1.3×10^3	770	0.06	7.4	Bis-Tris	*e*
3.4×10^4	9×10^3	4×10^3		400	4	7.5	HEPES	*f*
				IHP				
1×10^6					5	7.4	Bis-Tris	*b*
2×10^7				1×10^5	0.008	7.3	Bis-Tris	*g*
1.7×10^7				1.1×10^4	8 μM/1 mM	7.3	Bis-Tris	*c*
2.4×10^7				2.0×10^3	0.06	7.4	Bis-Tris	*e*
4.1×10^6	6×10^5	3×10^5		1.6×10^3	4	7.5	HEPES	*f*

[a] Temperature 20–25 °C, 0.1–0.12 M Cl$^-$, [buffer] = 0.05–0.1 M (λ values, M^{-1}; [heme], mM unless otherwise noted). [b] Nelson et al. (1974). [c] Benesch et al. (1977). [d] Hamasaki and Rose (1974). [e] Imaizumi et al. (1979). [f] Present study. [g] Edalji et al. (1976).

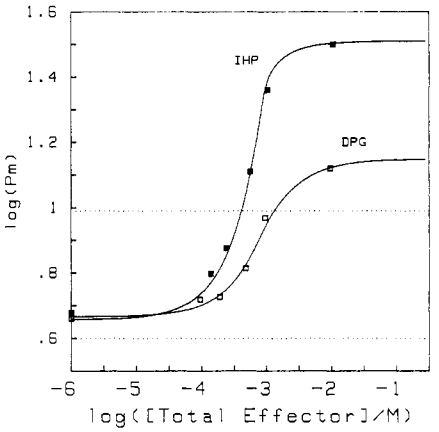

FIGURE 8: Dependence of the median oxygen partial pressure with limiting total amounts of effector. Smooth lines drawn with eq 18, 21, and 22 of the preceding paper and constants determined in simultaneous fits of DPG and IHP series. Points indicate the median values of the binding capacity experiments determined by numerical integration of each binding curve obtained by individual fitting. Dotted lines represent limiting values of the median obtained from the low hemoglobin concentration studies of Kister et al. (1987a) for zero and "infinite" DPG concentrations.

HEPES buffer rather than the Bis-Tris buffer used by Imaizumi et al. together with the fact that the tabulated values are apparent binding constants which therefore include effects of binding of any anionic or zwitterionic species present in the experimental conditions chosen. A similar discrepancy appears in the case of IHP for the deoxy and fully oxygenated species. Another source of disagreement may be the lower concentrations of hemoglobin used in the study of Imai et al. (1979), which are avoided in the present study.

We show in Figure 8 a plot of the median values observed in our experiments [determined from each individually fit binding curve by numerical integration [see Wyman (1964)]]. The smooth curves in this figure are drawn by using eq 18, 20, and 21 of the preceding paper, with constants determined from the simultaneous fitting of all experiments with either DPG or IHP. Through this plot we are able to compare in a broad way the results of our experiments, run at nearly physiologically high concentrations of Hb, with the results of the dilute Hb experiments of Kister et al. (1987a) for the case of DPG. The two horizontal lines in Figure 8 are the median values obtained by Kister et al. with no DPG (lower line) and saturating amounts of DPG (upper line), to be compared with the asymptotic values of the median curve for DPG obtained in our study. The deviations seen between the two studies are quite marked, with a higher oxygen affinity seen throughout the studies of Kister et al. The reason for this is perhaps increased dimer–tetramer equilibrium [see, for example, Ackers et al. (1975)] in those studies, which may be increased even more by DPG (Benesch et al. 1986).

Linkage of Effector Binding to Oxygen Binding. An easily measured quantity for the case of limiting effector is the change of oxygen saturation with a change of total effector in the system, obtained from binding curves taken at different total effector concentrations. A result of linkage thermodynamics shown in the preceding paper is that this quantity is identical with minus the change in effector chemical potential resulting from a change in oxygen chemical potential given a total amount of effector. This derivative itself represents the amplification or transduction efficiency of the macromolecule in the role of changing one ligand "signal" (change in chemical potential) into another. Integration of this function with respect to the logarithm of the oxygen partial pressure, plotted versus log pO_2, enables one to see the free effector concentration throughout the oxygen binding curve, which varies over more than an order of magnitude on a molar scale for low DPG/Hb ratios used in these experiments (not shown). The same behavior can be seen by using eq 10 of the preceding paper. For DPG concentrations much higher than equimolar with hemoglobin, the free DPG activity is essentially constant.

An examination of the variations of free energy changes of effector binding to hemoglobin as a function of the oxygenation step i ($-RT \ln \lambda_{i1}$) provides a visualization of the changes occurring in the macromolecule itself as oxygenation proceeds. In this way the effector acts as a probe of the structure of the macromolecule. Especially with the tightly binding effector IHP, the linkage of oxygen binding to binding of the effector occurs most strongly between binding the second and the last oxygen molecules, with smaller decreases in affinity for the preceding two steps. Although with DPG binding the error associated with the binding of effector to the doubly oxygenated intermediate is rather large, the difference in best-fit binding free energies of DPG and IHP at the different oxygenation states reveals essentially no change in the ability of the hemoglobin molecule to distinguish between these two effectors ($\Delta\Delta G \approx 3$ kcal/mol) until after the second oxygen is bound. The macromolecule then becomes far less discriminating (1 kcal/mol). Given the central location of the effectors' binding site, such a phenomenon may indicate partial obstruction of the effector binding site after the second oxygen is bound, perhaps by a large-scale conformational change of the hemoglobin tetramer. This possibility is implied as well by a qualitative study of the heats of carbon monoxide binding to human hemoglobin (Parody-Morreale et al., 1987).

Interpretation with the Truncated Allosteric Model. The truncated allosteric model invokes a quaternary conformational change of the hemoglobin molecule after the second oxygen is bound (Di Cera et al., 1987a). The marked change in the

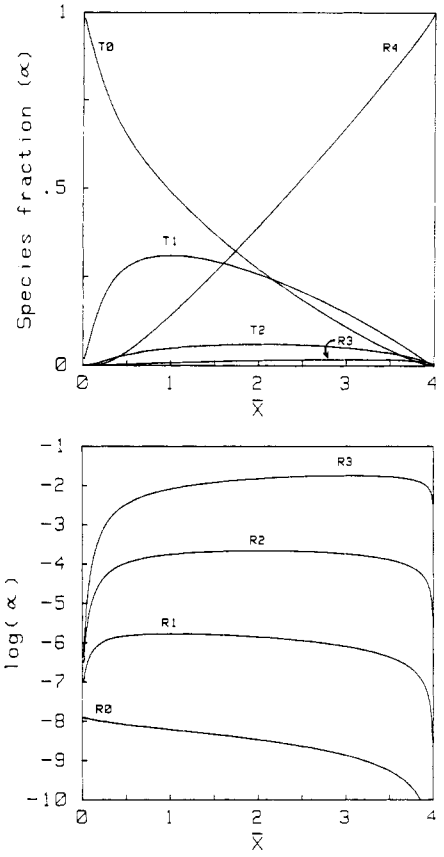

FIGURE 9: Top: Relative populations (species fractions) of major intermediate species in the course of oxygenation of human hemoglobin tetramers, as hypothesized by the truncated allosteric model, plotted versus average degree of ligation $\bar{X}$ ($\bar{X} = 4\theta$). Bottom: Logarithms of minor species fractions plotted versus $\bar{X}$.

effector binding properties of the hemoglobin tetramer after the second oxygen is bound thus prompted us to fit this model to the experimental data as shown under Results. The fit of this model to the experimental data is excellent, with essentially 100% confidence that the model is able to represent the data as well as the phenomenological Adair scheme for both effectors. With this model, the sudden shift in the observed binding properties of the effectors is interpreted as the conformational change of the Hb that is required after two oxygens are bound in order for ligation of the hemoglobin with oxygen to continue. The requirement that this transition occur before the third oxygen can bind is a key feature that leads to the low population of the triply ligated species.

In terms of significant populations of species, the truncated allosteric model, although encompassing two quaternary states, is practically a sequential binding model. A plot of the species fractions (α) for the model is shown in Figure 9. The populations of the R, RX, and RX_2 species of the allosteric model are essentially absent in the plot at the top of Figure 9, and the principal species are the unligated T, the TX, and the TX_2 species and the fully ligated molecule RX_4. Before the third oxygen binding reaction no major conformational changes take place, and the binding is characterized almost exclusively by the α chains in the T state since the allosteric constant L is so high as to prevent mixing in of the R state even at the second oxygen binding step. This mechanism is remarkably similar to one proposed by Perutz (1970). Because the populations of the intermediate R state species are small, an enlarged view of the behavior of these "minor species" is shown in the lower panel of Figure 9. The larger the values of L and κ_R, the less populated these minor species become. The model can thus be approximated by the sequence

$$\text{unligated T} \rightarrow \text{TX} \rightarrow \text{TX}_2 \rightarrow \text{RX}_3 \rightarrow \text{RX}_4$$

The third ligand binds with a concomitant conformational change that must occur to make room for the oxygen at the β-hemes, so that after this point the molecule is exclusively in the R state. With this approach to describing the truncated model, one can see easily that the low population of the triply oxygenated species is simply caused by the relatively unfavorable conformational change required to bind ligand to the β chains.

In attempting to explain the unique characteristics of hemoglobin, particularly those involving the triply oxygenated species, we have invoked the truncated allosteric model. This model is based on distinct structural features of the hemoglobin molecule that imply specific reaction properties of the α and β chains and elaborates on the two-state Monod–Wyman–Changeux model (Monod et al., 1965). The MWC model, while perhaps too simple to explain detailed behavior of such systems, nevertheless serves in a role analogous to that of the ideal gas model, that is, a starting point for mechanistic interpretation. A different philosophy is manifest where quaternary structural information plays a minor role and instead free energies of assembly are employed for the various intermediate oxidation states (Smith & Ackers, 1985) or metal-substituted hybrids (Smith et al., 1987) of hemoglobin, giving rise to a three-state "combinatorial switch" model (Smith & Ackers, 1985; Ackers & Smith, 1987). The latter is essentially a phenomenological description of the detailed thermodynamics of all the intermediates of these oxidation or metal-substitution processes. The problem of relating this approach to the essentially physiological ligation processes we have investigated requires that parallel studies be somehow made employing ligands such as oxygen or carbon monoxide.

ACKNOWLEDGMENTS

We thank Bo Hedlund (University of Minnesota) for providing us with hemoglobin samples used in this study. C.H.R. thanks Michael Doyle for pointing out work concerning the spectral effects of IHP binding.

Registry No. DPG, 138-81-8; IHP, 83-86-3; oxygen, 7782-44-7.

REFERENCES

Ackers, G. K. (1979) *Biochemistry 18*, 3372–3380.
Ackers, G. K., & Smith, F. R. (1987) *Annu. Rev. Biophys. Biophys. Chem. 16*, 583–609.
Ackers, G. K., Johnson, M. L., Mills, F. C., Halvorson, H. R., & Shapiro, S. (1975) *Biochemistry 14*, 5128–5134.
Adair, G. S. (1925) *J. Biol. Chem. 63*, 529–535.
Adams, M. L., & Schuster, T. M. (1974) *Biochem. Biophys. Res. Commun. 58*, 525–531.
Arnone, A. (1972) *Nature (London) 237*, 146–149.
Arnone, A., & Perutz, M. F. (1974) *Nature (London) 249*, 34–36.
Benesch, R., Benesch, R. E., & Yu, C. I. (1968) *Proc. Natl. Acad. Sci. U.S.A. 59*, 526–532.
Benesch, R. E., Benesch, R., Renthal, R., & Gratzer, W. B. (1971) *Nature (London), New Biol. 234*, 174–176.
Benesch, R., Edalji, R., & Benesch, R. E. (1977) *Biochemistry 16*, 2594–2597.
Benesch, R., Benesch, R., & Kwong, S. (1987) *J. Mol. Biol. 190*, 481–485.
Di Cera, E., Robert, C. H., & Gill, S. J. (1987a) *Biochemistry 26*, 4003–4008.

Di Cera, E., Doyle, M. L., Connelly, P. R., & Gill, S. J. (1987b) *Biochemistry 26*, 6494–6502.
Di Cera, E., Gill, S. J., & Wyman, J. (1988) *Proc. Natl. Acad. Sci. U.S.A. 85*, 449–452.
Dolman, D., & Gill, S. J. (1978) *Anal. Biochem. 87*, 127–134.
Doyle, M. L., Di Cera, E., Robert, C. H., & Gill, S. J. (1987) *J. Mol. Biol. 196*, 927–934.
Edalji, R., Benesch, R. E., & Benesch, R. (1976) *J. Biol. Chem. 251*, 7720–7721.
Gill, S. J., Di Cera, E., Doyle, M. L., Bishop, G. A., & Robert, C. H. (1987) *Biochemistry 26*, 3995–4002.
Gupta, R. K., Benovic, J. L., & Rose, Z. B. (1979) *J. Biol. Chem. 254*, 8250–8255.
Hamasaki, N., & Rose, Z. B. (1974) *J. Biol. Chem. 249*, 7896–7901.
Hayashi, A., Suzuki, T., & Shin, M. (1973) *Biochim. Biophys. Acta 310*, 309–316.
Herzfeld, J., & Stanley, H. E. (1974) *J. Mol. Biol. 82*, 231–265.
Imai, K., & Tyuma, I. (1973) *Biochim. Biophys. Acta 293*, 290–294.
Imaizumi, K., Imai, K., & Tyuma, I. (1978) *J. Biochem. (Tokyo) 83*, 1707–1713.
Imaizumi, K., Imai, K., & Tyuma, I. (1979) *J. Biochem. (Tokyo) 86*, 1829–1840.
Jänig, G. R., Ruckpaul, K., & Jung, F. (1971) *FEBS Lett. 17*, 173–176.
Johnson, M. L. (1981) *Biophys. J. 44*, 101–106.
Johnson, M. L., & Ackers, G. K. (1977) *Biophys. Chem. 7*, 77–80.
Kilmartin, J. V., Imai, K., Jones, R. T., Faruqui, A. R., Fogg, J., & Baldwin, J. M. (1978) *Biochim. Biophys. Acta 534*, 15–25.
Kister, J., Poyart, C., & Edelstein, S. J. (1987a) *J. Biol. Chem. 262*, 12085–12091.
Kister, J., Poyart, C., & Edelstein, S. J. (1987b) *Biophys. J. 52*, 527–535.
Magar, M. E. (1972) *Data Analysis in Biochemistry and Biophysics*, Academic, New York.
Marquardt, D. W. (1963) *J. Soc. Ind. Appl. Math. 11*, 431–444.
Monod, J., Wyman, J., & Changeux, J. P. (1965) *J. Mol. Biol. 12*, 88–118.
Nelson, D. P., Miller, W. D., & Kiesow, L. A. (1974) *J. Biol. Chem. 249*, 4770–4775.
Parody-Morreale, A., Robert, C. H., Bishop, G. A., & Gill, S. J. (1987) *J. Biol. Chem. 262*, 10994–10999.
Perella, M., Kilmartin, J. V., Fogg, J., & Rossi-Bernardi, L. (1975) *Nature (London) 256*, 759–761.
Perutz, M. F. (1970) *Nature (London) 228*, 726–739.
Robert, C. H., Decker, H., Richey, B., Gill, S. J., & Wyman, J. (1987) *Proc. Natl. Acad. Sci. U.S.A. 84*, 1891–1895.
Robert, C. H., Gill, S. J., & Wyman, J. (1988) *Biochemistry* (preceding paper in this issue).
Smith, F. R., & Ackers, G. K. (1985) *Proc. Natl. Acad. Sci. U.S.A. 82*, 5347–5351.
Smith, F. R., Gingrich, D., Hoffman, B. M., & Ackers, G. K. (1987) *Proc. Natl. Acad. Sci. U.S.A. 84*, 7089–7093.
Spokane, R. B., Brill, R. V., & Gill, S. J. (1980) *Anal. Biochem. 109*, 137–145.
Sturgill, T., & Biltonen, R. L. (1976) *Biopolymers 15*, 337–354.
Szabo, A., & Karplus, M. (1976) *Biochemistry 15*, 2869–2877.
Tyuma, I., Imai, K., & Shimuzu, K. (1973) *Biochem. Biophys. Res. Commun. 44*, 682–686.
Williams, R. C., & Tsay, K. (1973) *Anal. Biochem. 54*, 137–145.
Wyman, J. (1948) *Adv. Protein Chem. 4*, 407–531.